PNAS
www.pnas.org

Supplementary Information for

Transcriptome-based design of antisense inhibitors potentiates carbapenem efficacy in CRE Escherichia coli

Thomas R. Aunins, Keesha E. Erickson, and Anushree Chatterjee

Anushree Chatterjee
Email: chatterjee@colorado.edu

This PDF file includes:

Supplementary methods and results
Figures S1 to S15
Tables S1 to S6
SI References

Other supplementary materials for this manuscript include the following:

Datasets S1 to S2

Supplementary Information Text

Sequence typing. *Escherichia coli* strains do not cluster cleanly into phylogenic trees. For instance, non-pathogenic and pathogenic strains appear in each of the four main groups (A, B1, B2, and D), and even the specific pathogenic type, such as enterohaemorrhagic (EHEC), enteropathogenic (EPEC), and enteroinvasive (EIEC) *E. coli* is dispersed among phylogenetic groups (1). Heterogeneity among phylogenetic groups has been speculated to be due to high levels of recombination or to rapid radiation after bottlenecking (1). Nevertheless, information useful in characterization can be obtained by determining sequence type and phylogenetic grouping. We used the draft genome assembly to classify *E. coli* CUS2B per the MultiLocus Sequencing Typing (MLST 1.8) tool from the Center for Genomic Epidemiology (2). We employed the MLST from Jaureguy et. al.,(3) which determines type using the sequence of eight housekeeping genes. By this scheme, the isolate was found to match ST-44 in phylogenetic group D. Group D has found to have higher mutation rates as a whole when compared to other groups, but is itself a diverse group, with members including K1, EHEC, EIEC, Shigella, other pathogens, and non-pathogenic strains (1).

Analysis of mutations contributing to fluoroquinolone, rifampicin, or nitrofurantoin resistance. We did not identify any antibiotic resistance genes that could impart fluoroquinolone, rifampicin, or nitrofurantoin resistance, so we searched the genome sequence for mutations known to convey resistance to these antibiotics (Table S3). Comparing the sequence of CUS2B to that of the antibiotic-susceptible strain *E. coli* MG1655, we find codon changes at positions 83 and 87 in the DNA gyrase subunit A gene *gyrA*; mutations in these positions have been previously revealed to result in fluoroquinolone resistance (4). There were four codon changes in DNA gyrase subunit B (*gyrB*). None of the four positions fell in a resistance-determining region (5), though it has been suggested that *gyrA* mutations are more frequent and bestow a selective advantage for fluoroquinolone resistance in *E. coli* (6). There were five codon changes identified in *nfsA* and three in *nfsB*, NADPH nitroreductase genes that are nitrofurantoin resistance determinants. None of the eight positions matched those from previous studies analyzing the genetic basis for nitrofurantoin resistance (7, 8), however, the wide range of resistance-conferring mutations previously identified suggests that there may not be a narrow resistance-determining region in *nfsA/B*. We did not find any nonsynonymous mutations in *rpoB*, which is a determinant of rifampicin resistance (9). Thus, the low-level rifampicin resistance observed may be a result of either a non-specific antibiotic response, or mutations in other genes not commonly linked to rifampicin resistance.

Antisense RNA involved in carbapenem-resistance. In this analysis, we located antisense RNA that were DE in response to ertapenem and meropenem treatment and summarized the potential functions that these RNAs could influence via antisense binding (Fig. S3). The percentage of differentially expressed antisense transcripts ranged between 4% (in ertapenem at 60 minutes) and 23% (in meropenem at 60 minutes) of the total number of transcripts (Fig. S3A). More antisense transcripts were significantly upregulated than downregulated in all cases, and no downregulated antisense transcripts were identified in either ertapenem or meropenem at 60 minutes. We grouped the antisense transcripts identified in ertapenem or meropenem by the biological function of the sense gene (Fig. S3B). The plurality of these corresponding sense genes did not have a known function (31% in ertapenem, 47% in meropenem). Of the genes with known function, we find functions related to transport, metabolism, oxidation-reduction, protease, and transcriptional regulation. Functions unique to upregulated transcripts in ertapenem include amino acid processing, DNA processing, membrane, signal transduction, and stress response. Two antisense transcripts were DE only in ertapenem, at both 30 and 60 min (Fig. S3C). *psiE* is associated with stress response, while the BTW13_RS28340 is of unknown function, and each was upregulated with respect to the no treatment condition. Two other transcripts were significantly upregulated in ertapenem at 30 and 60 minutes, in meropenem at 30 minutes, but not in meropenem at 60 minutes. One of these is antisense to the regulator *zur* and the other, BTW13_RS03075, is of unknown function (Fig. S3C).

Gel shift mobility assay. Single-stranded DNA oligonucleotides (Integrated DNA Technologies), comprising 60 nucleotides from the target region of each gene (Table S6), were incubated overnight at 4ºC with their respective PNA sequence (synthesized without cell-penetrating peptide) in 1X TE buffer with 20 mM KCl (pH 7.0). Additionally, PNA were incubated with a corresponding oligonucleotide with two nucleotide mismatches in the 12-base PNA target sequence, as a control (Table S6). Oligonucleotide concentration for the incubation was 500 nM, while the PNA concentration was estimated to be at least 5 µM, based on the absorbance of the crude sample. PNA-ssDNA binding was monitored on a 12% polyacrylamide non-denaturing gel using 1X TBE as a running buffer (pH 8.0). SYBR® Gold Nucleic Acid Gel Stain (Invitrogen) was used to visualize the nucleotide bands in the gel. The gel was imaged using a Gel Doc™ EZ Imager (Bio-Rad) with a UV sample tray.

GFP knockdown PNA assay. Three colonies were picked from a plate of *E. coli* DH5αZ1 expressing GFP, and were used to inoculate three separate overnight cultures in 1 mL CAMHB each. After 16 hours, the culture was diluted 1:10,000 in a 384-well microplate using three biological replicates per condition. The cultures were treated with a 0.01 mM IPTG to induce fluorescence, and with the PNA *α-GFP* at 10 µM (Table S5). Additional conditions were also treated with 0.01 mM IPTG and either scrambled or mismatched versions of the inhibitor PNA (named *scr-GFP* and *2MM-GFP*, respectively) as controls. The total culture volume for each treatment was 50 µL. The cultures were grown at 37ºC with shaking for 24 hours. Then, each culture was transferred to a conical plate and centrifuged at 4,000 rpm for 5 minutes to pellet the cells. The supernatant was removed and the cells were washed with phosphate buffered saline (PBS) and pelleted once more in the centrifuge. The cells were then re-suspended in PBS and measured for both fluorescence (excitation wavelength: 485 nm, emission wavelength: 562 nm) and optical density (590 nm). Fluorescence for each well was normalized to optical density.

Keio knockout strain PNA assays. Three colonies were picked from each respective Keio knockout plate and used to inoculate three separate overnight cultures in 1 mL CAMHB each. After 16 hours, the culture was diluted 1:10,000 in a 384-well microplate using three biological replicates per condition. PNA corresponding to each strain's knocked-out gene was added to the cultures for a final concentration of 10 µM. The total culture volume for each treatment was 50 µL. Growth in the plate was monitored with a Tecan GENios (Tecan Group Ltd.) plate reader running Magellan™ software (v 7.2) at an absorbance of 590 nm every 20 minutes for 20 hours, with shaking between measurements.

Colony-forming unit assay. *E. coli* CUS2B was grown and treated according to the conditions specified in the main text Methods section under the subheading "PNA-antibiotic growth curve interaction assays." At the end of the 24-hour treatment period, each replicate was serially diluted in PBS. 10 uL of each dilution was plated on a solid CAMHB plate (with 15 g/L agar and 100 µg/mL ampicillin) and allowed to run down. The colonies were incubated at 37ºC for 16 hours prior to counting.

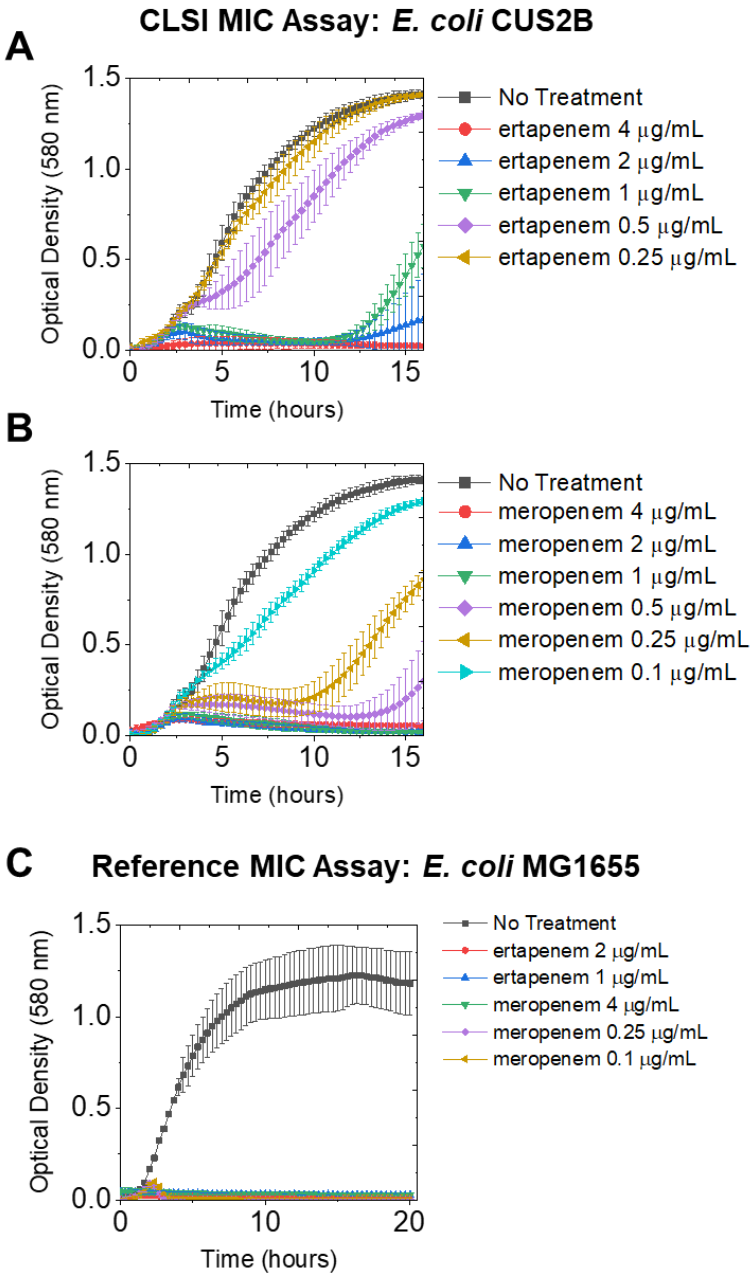

Fig. S1. Growth curves for *E. coli* CUS2B treated for 16 hours with the (A) ertapenem and (B) meropenem in serial twofold dilutions of each antibiotic. Minimum inhibitory concentration was determined using procedures published by the Clinical and Laboratory Standards Institute (10) (See main text Methods). (C) For comparison, the assay was also run for relevant concentrations of the carbapenems (the *E. coli* CUS2B MICs and the CLSI breakpoints) with reference strain *E. coli* MG1655.

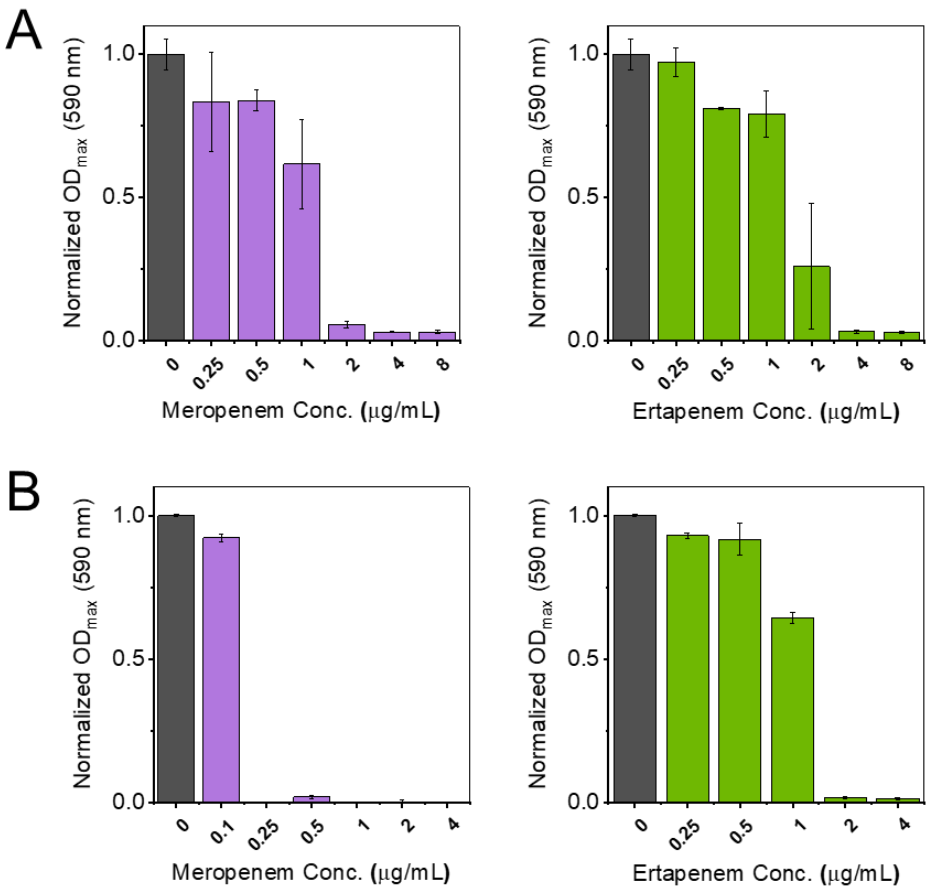

Fig. S2. Minimum inhibitory concentrations for experimental conditions. (A) Maximum optical density (590 nm) for each antibiotic concentration, normalized to an untreated control. Growth conditions here are as in the RNA-seq experiment: a 1:20 dilution from an overnight culture was grown for 1 hour before the addition of antibiotics. (B) 24-hour endpoint optical density (590 nm) for each antibiotic concentration, normalized to an untreated control. Growth conditions here are as in the antibiotic-PNA interaction experiments: a 1:10,000 dilution from an overnight culture was treated with antibiotic and grown for 24 hours.

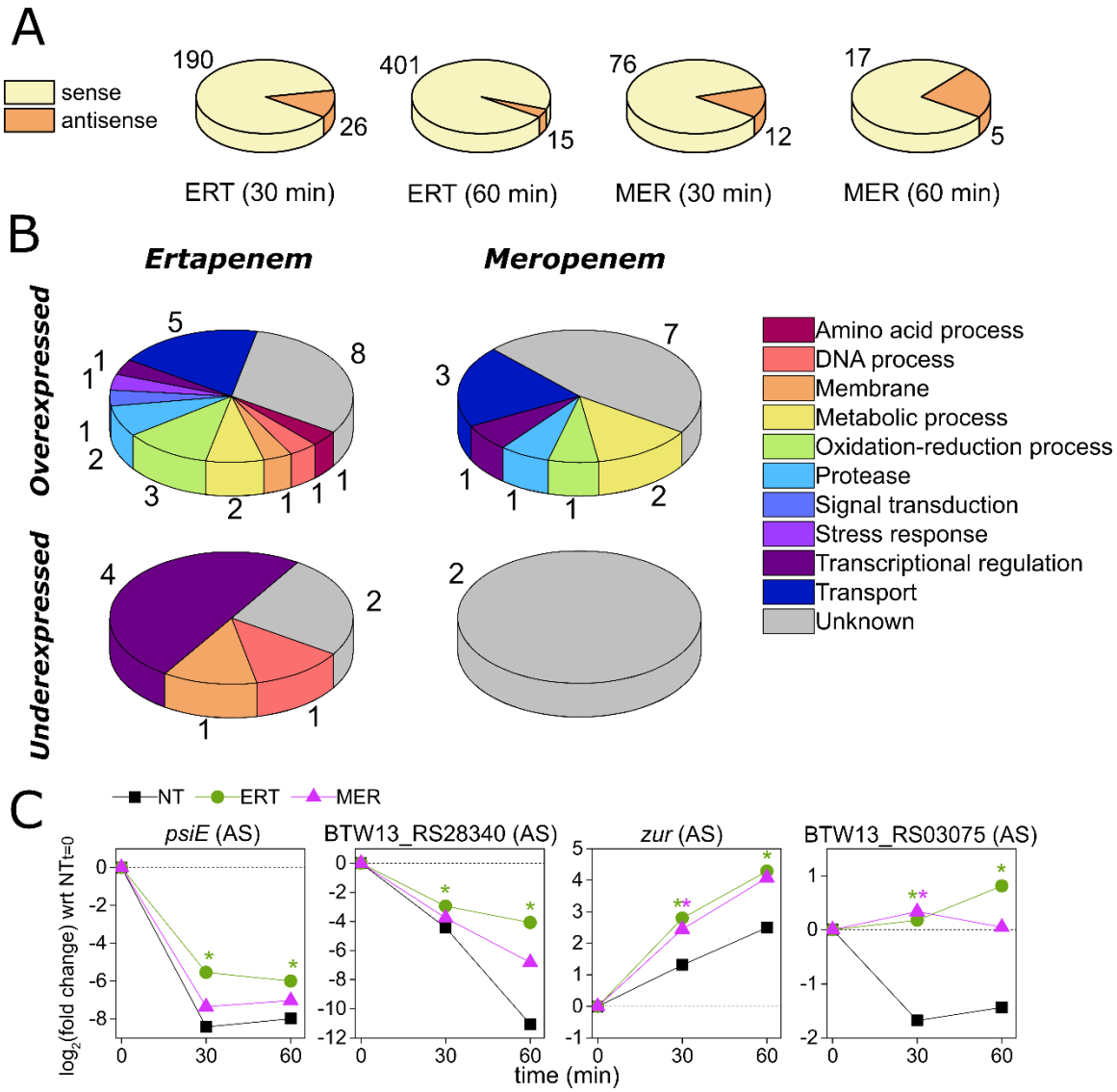

Fig. S3. (A) Percentage of differentially expressed sense and antisense transcripts in each experimental condition. Number of transcripts in each case is indicated. (B) Percentage of differentially expressed antisense transcripts, by functional class. Transcripts from 30 and 60 minutes are grouped together for this analysis, within their respective antibiotic treatment category. (C) Time course of four antisense transcripts of interest. Log_2(fold change) here is with respect to the no treatment condition at time t = 0. NT = no treatment, ERT = ertapenem, MER = meropenem.

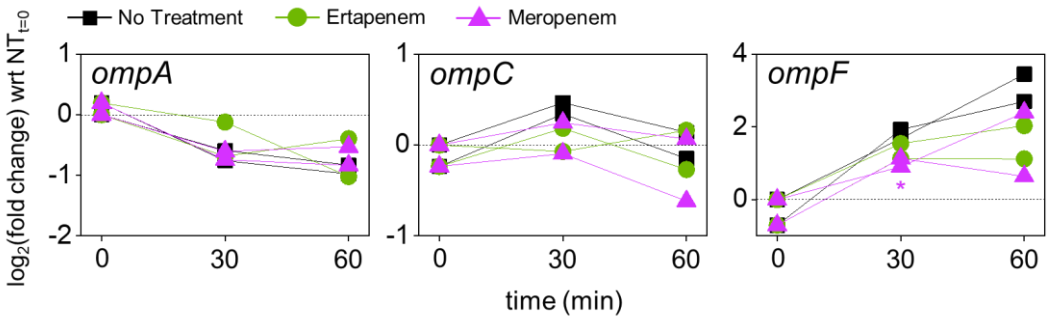

Fig. S4. Time course of gene expression for the outer membrane porin genes *ompA*, *ompC*, and *ompF*. All conditions are normalized to the 0-minute timepoint expression levels of one biological replicate, just before antibiotic treatments were introduced. Asterisks indicate significant DE ($q < 0.05$). NT = no treatment.

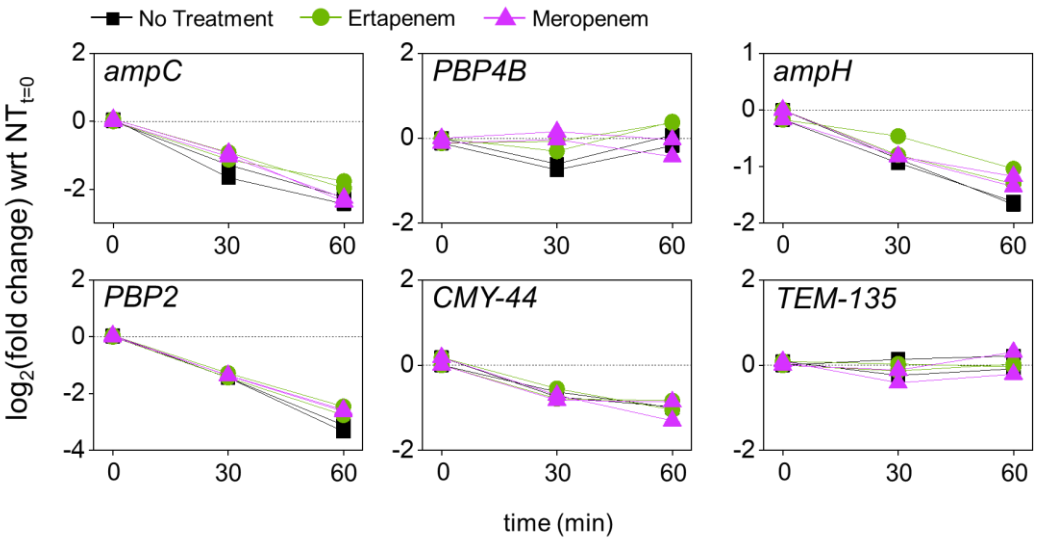

Fig. S5. Time course of gene expression for the β-lactam-related genes encoded by *E. coli* CUS2B. All conditions are normalized to the 0-minute timepoint expression levels of one biological replicate, just before antibiotic treatments were introduced. None of these genes were significantly differentially expressed with respect to the no treatment samples at the same timepoint. NT = no treatment.

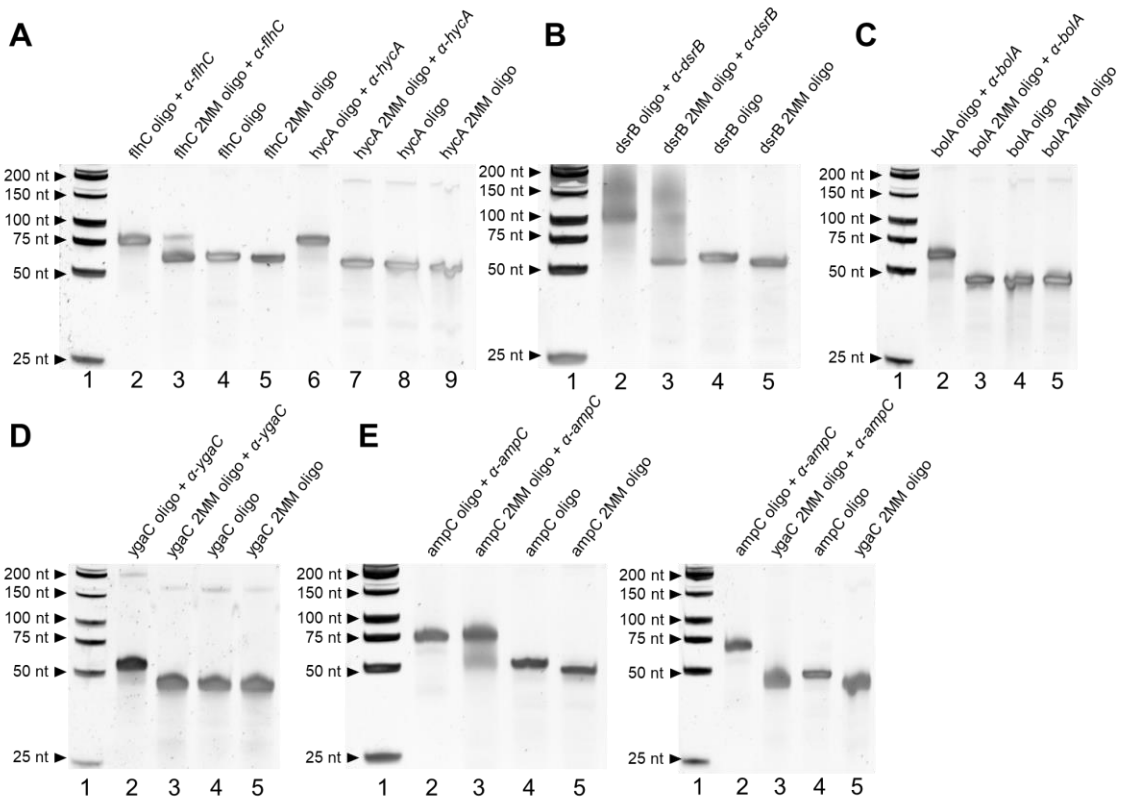

Fig. S6. Gel shift mobility assay for PNA-ssDNA binding. PNAs (without CPP and linker residue) were incubated with a 60nt ssDNA oligonucleotide containing either a perfectly matched target sequence or a two-mismatch (2MM) target sequence. These samples were run in a polyacrylamide gel shift assay and stained with SYBR Gold stain to demonstrate binding. Oligonucleotides with PNA bound will show bands shifted higher in the gel, as PNA inhibit their mobility through the gel due to both an increase in size and decrease in charge-to-mass ratio (PNA are uncharged). Lane 1 in each gel image is a low molecular weight ssDNA ladder. In panel A, lanes 2 and 6 contain PNAs incubated with perfectly matched oligonucleotides, lanes 3 and 7 contain PNAs incubated with 2MM oligonucleotides, and lanes 4/5 and 8/9 contain the same oligonucleotides without PNA. In the remaining panels, lane 2 contains PNA with its perfectly matched oligonucleotide, lane 3 contains PNA with its 2MM oligonucleotide, and lanes 4/5 contain the oligonucleotides without PNA. The PNAs for which antibiotic interaction was observed were assayed: (A) α-*flhC* (lanes 2-5) and α-*hycA* (lanes 6-9) with respective matched and mismatched oligos, (B) α-*dsrB*, (C) α-*bolA*, (D) α-*ygaC*, and (E) α-*ampC*. As the PNA α-*ampC* shows some binding to its two-mismatch oligonucleotide, it is also shown in a gel with the two-mismatch ygaC oligonucleotide (E) to demonstrate that α-*ampC* does not bind generally to unmatched ssDNA sequences.

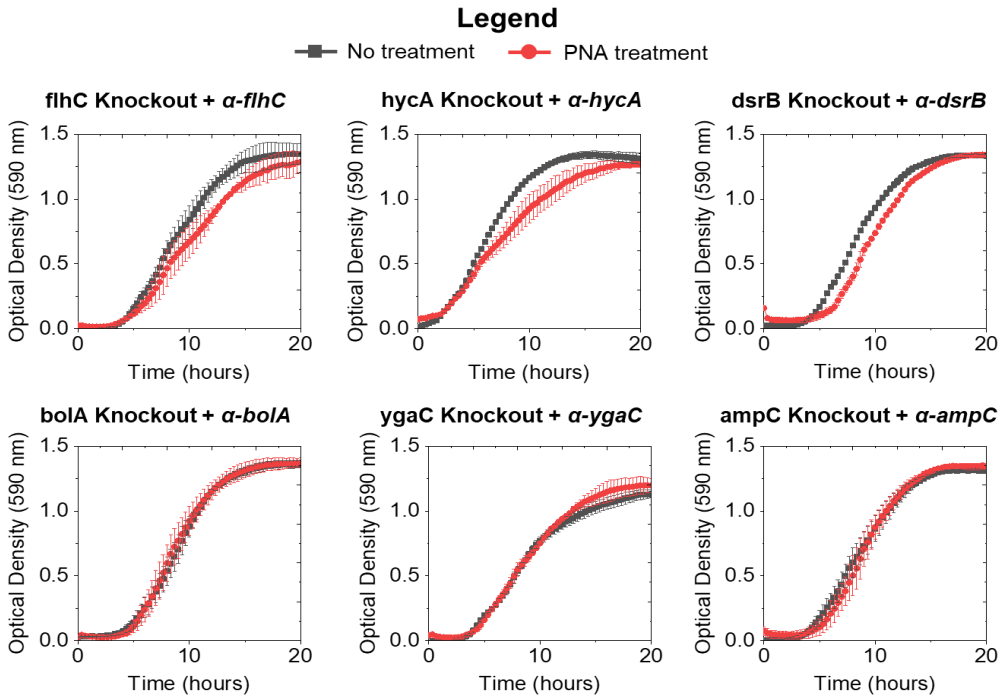

Fig. S7. Growth curves for *E. coli* Keio collection knockouts. Each knockout strain was treated with its corresponding anti-gene PNA and grown for 20 hours, to determine whether the PNA had non-specific growth effects. The assay was performed with three biological replicates for each condition.

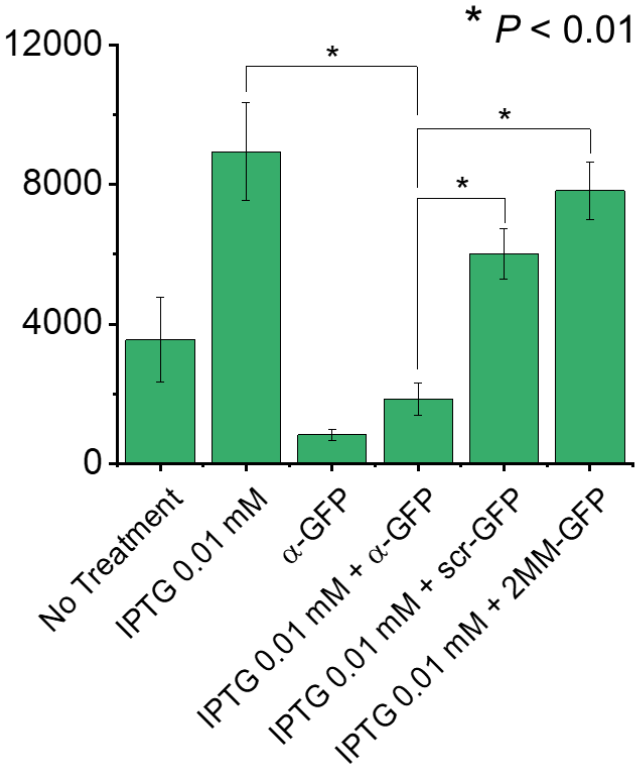

PNA Name	PNA Sequence (N to C)
α-GFP	**T**CCTTCTCTCCT
scr-GFP	TCCCCCTTTTTC
2MM-GFP	**T**CCCTCTTTCCT

Bold: Start codon
Red: Mismatch

Fig. S8. GFP fluorescence assay for PNA efficacy. A GFP-expressing strain of *E. coli* was diluted 1:10,000 from overnight and grown for 24-hours with IPTG at 0.01 mM to induce expression, as well as with one of three PNA at 10 μM: α-GFP (the anti-gene treatment), or a scrambled sequence or two-mismatch control (scr-GFP and 2MM-GFP, respectively). PNA sequences are shown in a table to the right, and in Table S5. The assay was performed with three biological replicates for each condition. The two control sequence treatments did not differ significantly ($P > 0.1$) from the positive control. *: $P < 0.01$.

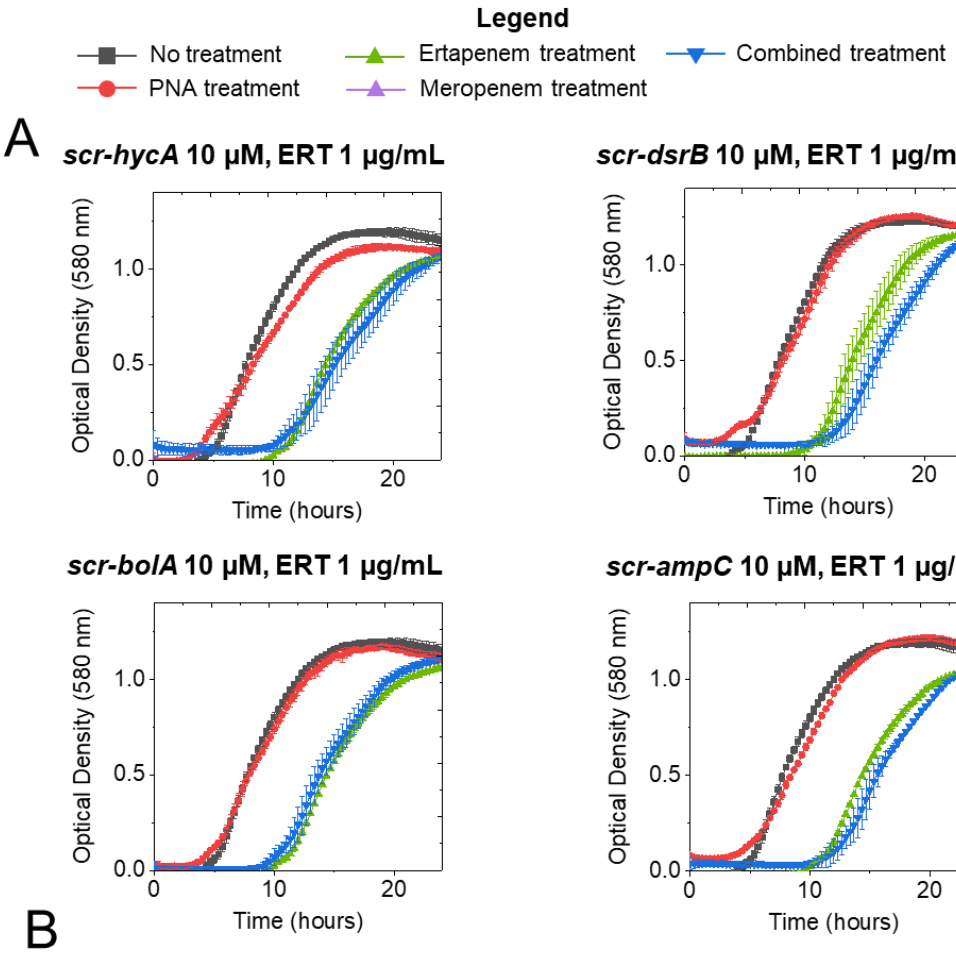

PNA Name	PNA Sequence (N to C)	Scrambled PNA Sequence
α-ampC	**CAT**AGGGTCTGG	ACGTGGGTCGTA
α-bolA	GTAT**CAT**CATGA	TTACATACAGTG
α-dsrB	TTTTTCTGG**CAG**	TTGTACTTGGCT
α-hycA	TAGT**CAT**TGTCA	TTACCGTTAGAT
2MM-ampC	**CAT**CGGGTATGG	n/a

Bold: Start codon
Red: Mismatch

Fig. S9. Scrambled sequence (scr) and two-mismatch (2MM) ertapenem controls. *E. coli* CUS2B was treated with a combination of a scrambled-sequence PNA (corresponding to each of the effective anti-gene PNA treatments) and ertapenem, for each condition in which significant interaction was observed with the anti-gene PNAs. PNA sequences are shown at the bottom of the figure. Each condition was measured in triplicate, and no interaction was observed.

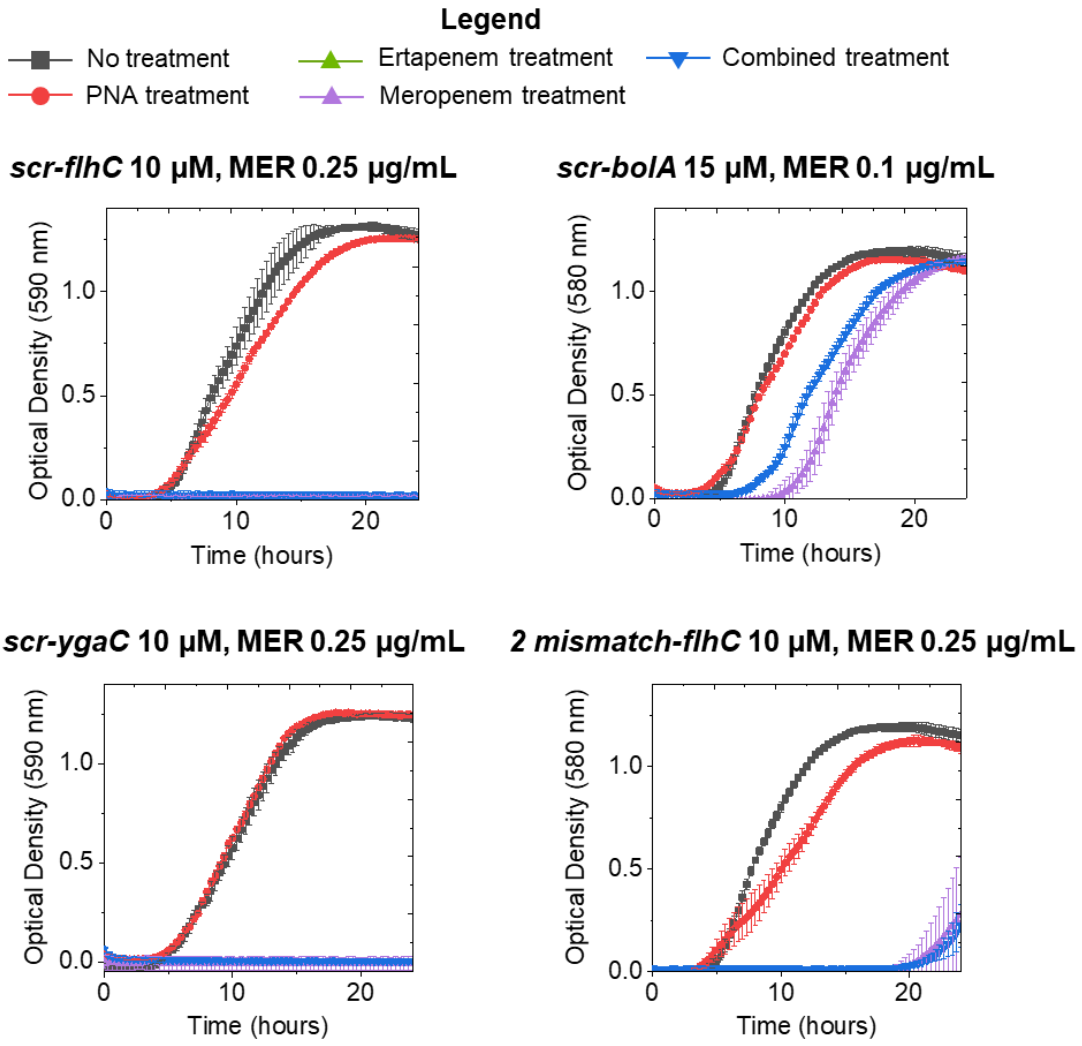

PNA Name	PNA Sequence (N to C)	Scrambled PNA Sequence
α-bolA	GTAT**CAT**CATGA	TTACATACAGTG
α-flhC	G**CAT**TATTCCCA	TCTATCTAGCAC
α-ygaC	ATA**CAT**ATTTGA	TTAGATATTAAC
2MM-flhC	G**CA**CTATTCCTA	n/a

Bold: Start codon
Red: Mismatch

Fig. S10. Scrambled sequence (scr) and two-mismatch (2MM) meropenem controls. *E. coli* CUS2B was treated with a combination of a scrambled-sequence PNA (corresponding to each of the effective anti-gene PNA treatments) and meropenem, shown for each condition in which significant interaction was observed with the anti-gene PNAs. PNA sequences are shown at the bottom of the figure. Each condition was measured in triplicate and no interaction was observed.

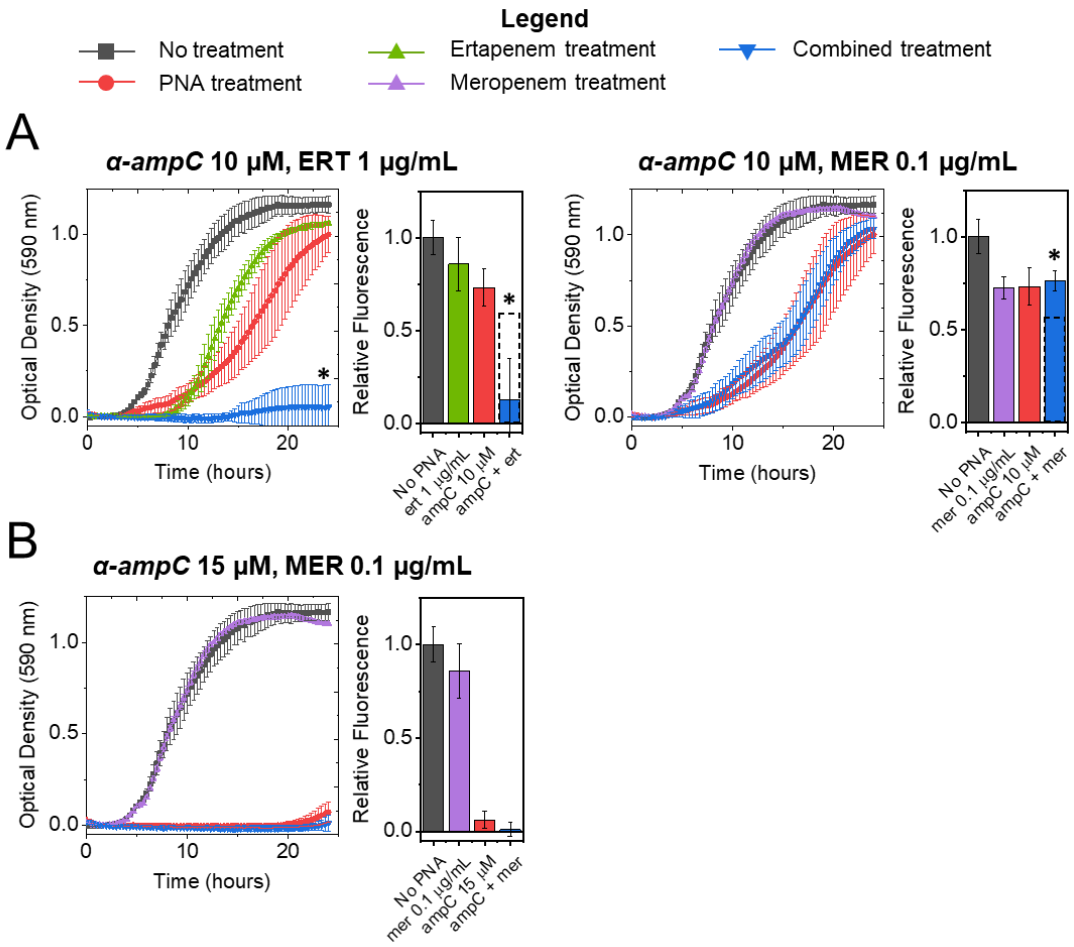

Fig. S11. Growth curves and cell viability assays for *E. coli* CUS2B treated with a combination or ertapenem or meropenem, each condition measured in triplicate. (A) α-*ampC* at 10 μM combined with ertapenem at 1 μg/mL and meropenem at 0.1 μg/mL. Significant synergistic interaction was observed in the growth curve endpoint and viability assay for α-*ampC* and ertapenem. Significant antagonistic interaction was observed in the α-*ampC* at 10 μM and meropenem combination, though it was not found in the growth curve endpoints. (B) α-*ampC* at 15 μM combined with meropenem at 0.1 μg/mL. No significant interaction was observed (two-way ANOVA, $P < 0.05$).

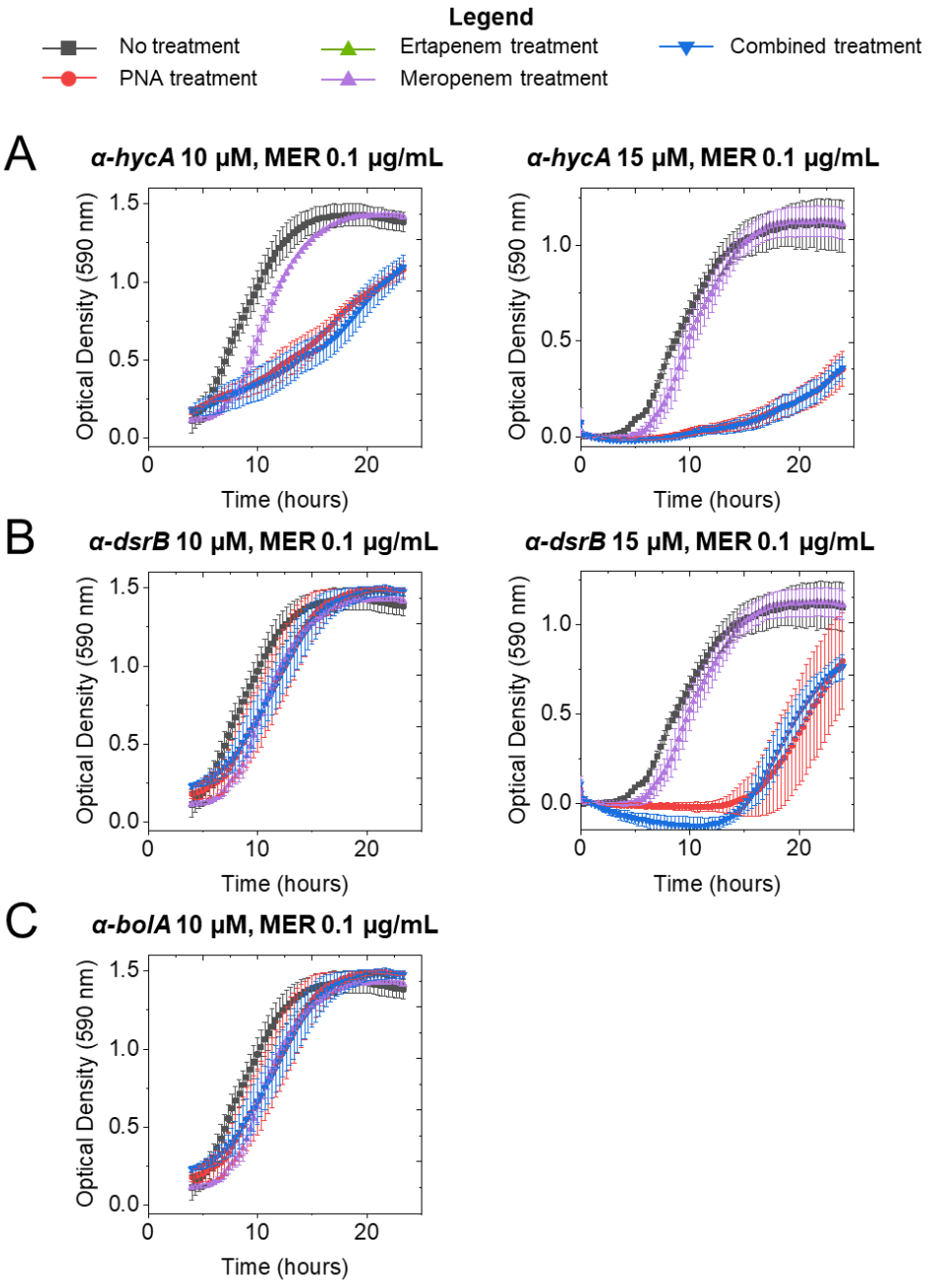

Fig. S12. Growth curves for *E. coli* CUS2B treated with a combination of (A) α-*hycA*, (B) α-*dsrB*, or (C) α-*bolA* at 10 μM and 15 μM, and meropenem at 0.1 μg/mL. Each condition was measured in triplicate and no significant interaction was observed (two-way ANOVA, $P < 0.05$). (Note: Though the cultures for the left-side panels were incubated with regular shaking for the first 4 hours of treatment, measurement data was lost. As such, growth curves are normalized by subtracting non-culture microplate wells containing broth, instead of subtracting early timepoints as with the main text data).

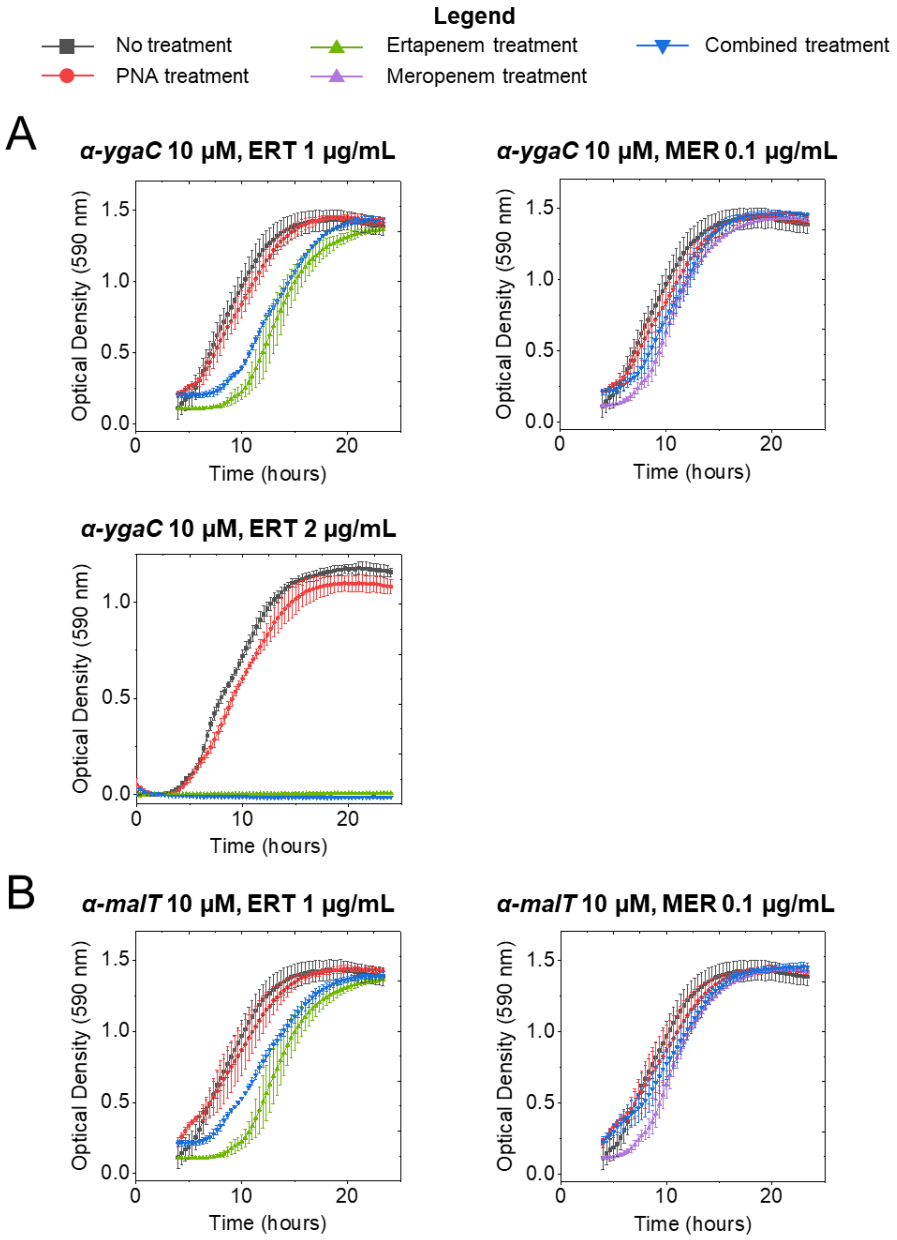

Fig. S13. Growth curves for *E. coli* CUS2B treated with a combination of (A) α-*ygaC* or (B) α-*malT* at 10 μM and carbapenem antibiotics (ertapenem at 1 or 2 μg/mL or meropenem at 0.1 μg/mL). Each condition was measured in triplicate. No significant interaction was observed (two-way ANOVA, $P < 0.05$), and these PNA were not pursued further in potentiating the carbapenems. (Note: Though the cultures were incubated with regular shaking for the first 4 hours of treatment, measurement data was lost. As such, growth curves are normalized by subtracting non-culture microplate wells containing broth, instead of subtracting early timepoints as with the main text data).

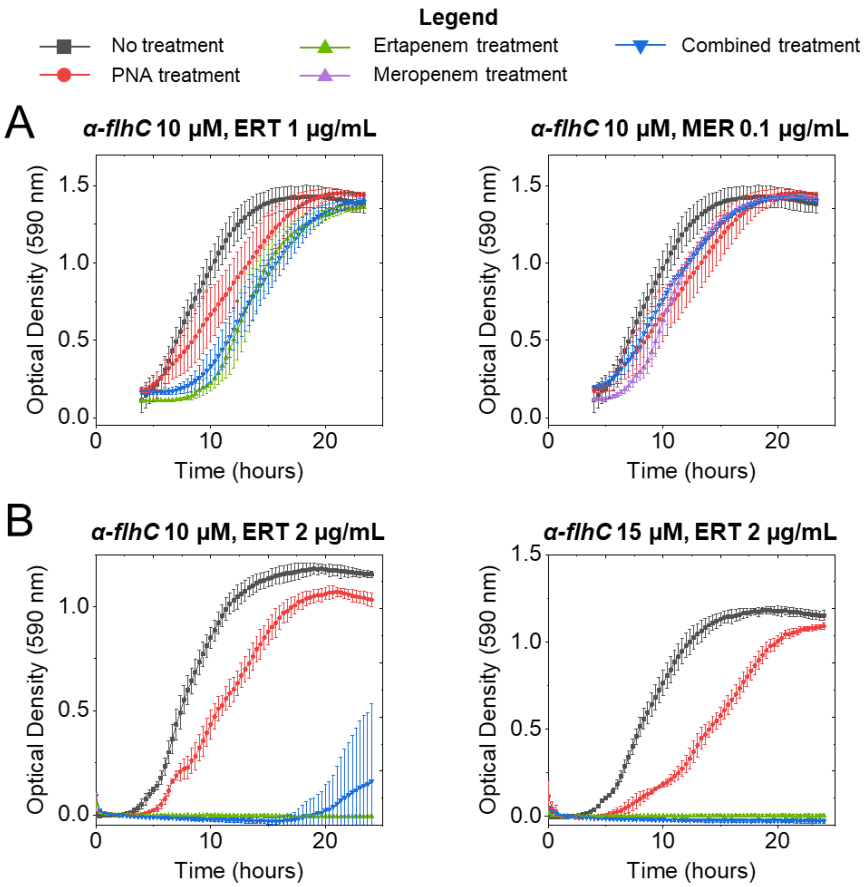

Fig. S14. (A) Growth curves for the α-*flhC*/carbapenem combinations at sub-MIC carbapenem concentrations. (B) Growth curves for the α-*flhC*/MIC ertapenem treatment growth rescue experiments. Each condition was measured in triplicate and no significant interaction was observed (two-way ANOVA, $P < 0.05$). (Note: Though the cultures for the top two panels were incubated with regular shaking for the first 4 hours of treatment, measurement data was lost. As such, growth curves are normalized by subtracting non-culture microplate wells containing broth, instead of subtracting early timepoints as with the main text data).

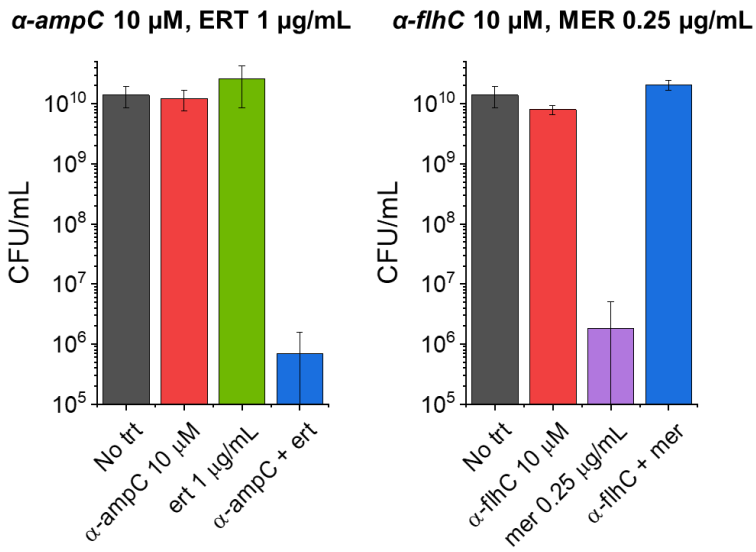

Fig. S15. Colony-forming units per milliliter for two PNA-antibiotic combinations for which significant interaction was observed, for comparison with resazurin viability assays. *E. coli* CUS2B was treated with each respective treatment for 24 hours before dilution and plating on solid CAMHB plates. Plated colonies were grown at 37ºC for 16 hours before counting. ERT = ertapenem, MER = meropenem.

Table S1. Comparison of four genes related to β-lactam resistance located in the genome of CUS2B with homologues in *E. coli* strain MG1655. Genes were identified using the ARG-ANNOT database.

***E. coli* CUS2B Gene ID**	**Homologue enzyme type**	***E. coli* MG1655 homologue**	**Nucleotide conservation, *E. coli* MG1655**	**Amino acid conservation, *E. coli* MG1655**	**Mutations vs MG1655**
BTW13_RS13915	β-lactamase	*ampC*	98%	97% (368 of 378)	T4M, S102I, T105A, E140D, Q196H, N201T, P209S, N260T, S298I, D367A
BTW13_RS14855	PBP	*yfeW* (PBP4B)	96%	99% (429 of 433)	V53A, S57G, N272D, T388A
BTW13_RS17910	PBP	*ampH*	96%	99% (385 of 386)	V83I
BTW13_RS17320	PBP	*mrdA* (PBP2)	99%	100% (634 of 634)	none

Table S2. Differentially expressed genes from select total RNA-seq overlap categories. ERT = ertapenem, MER = meropenem, Bold = motility-associated genes.

ERT 30 min. and MER 30 min. (41 genes)	ERT 30 min. and ERT 60 min. (38 genes)
alaE	*[citrate (pro-3S)-lyase] ligase*
bdm	*4-alpha-glucanotransferase*
bifunctional N-acetylglucosamine-1-phosphate uridyltransferase/glucosamine-1-phosphate acetyltransferase	*50S ribosomal protein L11*
EEP domain-containing protein	*alpha-glycosidase*
flagellar L-ring protein	*carbamoyl-phosphate synthase large chain*
flgA	*carbon starvation protein A*
flgC	*citrate (pro-3S)-lyase subunit beta*
flgD	*citrate lyase ACP*
flgE	*citrate lyase subunit alpha*
flgF	*degP*
flgG	*dihydroorotate dehydrogenase (quinone)*
flgI	*emrA*
flgJ	*formate hydrogenlyase complex iron-sulfur subunit*
flgK	*formate hydrogenlyase subunit 3*
flhA	*hycA*
flhB	*hycD*
fliA	*hycE*
fliD	*hydN*
fliF	*hypA*
fliG	*hypothetical protein (2)*
fliH	*lamB*
fliI	*loiP*
fliJ	*lptG*
fliK	*malE*
fliL	*malF*
fliM	*malG*
fliN	*malK*
fliO	*maltodextrin phosphorylase*
fliP	*membrane protein*
fliZ	*NADH dehydrogenase*
glutamine--fructose-6-phosphate aminotransferase	*phage shock protein C*
hypothetical protein (5)	*phage shock protein G*
IlvGMEDA operon leader peptide	*phoH*
N-acetylmuramic acid 6-phosphate etherase	*plaP*
pyruvate dehydrogenase complex repressor	*psiE*
stress-induced protein, UPF0337 family	*translation initiation factor*
transketolase	

Table S3. Codon changes in *E. coli* CUS2B as compared to MG1655 in genes associated with resistance to fluoroquinolones, nitrofurantoins, or rifampicin.

Gene	Nonsynonymous mutations vs MG1655	Associated resistance
gyrA	S83L, D87N	Fluoroquinolone
gyrB	A359E, T618A, A653T, V663I	
nfsA	F9C, D58E, K72Q, T117I, E141K	Nitrofurantoin
nfsB	D66G, V93A, E137Q	
rpoB	none	Rifampicin

Table S4. PNA targets and antisense PNA sequences. Each PNA sequence was coupled at the N terminus with a cell-penetrating peptide $(KFF)_3K$ and a 2-[2-(2-Aminoethoxy)ethoxy]acetyl linker group. Nucleotides in the start codon, as well as PNA bases that complement those nucleotides, are bolded, and mismatched nucleotides are shown in red.

PNA Name	Target (5' to 3')	PNA Sequence (N to C)	Scrambled PNA Sequence (N to C)
α-ampC	CCAGACCCT**ATG**	**CAT**AGGGTCTGG	ACGTGGGTCGTA
α-bolA	TCATG**ATG**ATAC	GTAT**CAT**CATGA	TTACATACAGTG
α-dsrB	**CTG**CCAGAAAAA	TTTTTCTGG**CAG**	TTGTACTTGGCT
α-flhC	TGGGAATA**ATG**C	G**CAT**TATTCCCA	TCTATCTAGCAC
α-hycA	TGACA**ATG**ACTA	TAGT**CAT**TGTCA	TTACCGTTAGAT
α-malT	GTGATTAACT**AT**	**AT**AGTTAATCAC	n/a
α-ygaC	TCAAAT**ATG**TAT	ATA**CAT**ATTTGA	TTAGATATTAAC
2MM-ampC	CCATACCCG**ATG**	**CAT**CGGGTATGG	n/a
2MM-flhC	TAGGAATA**GTG**C	G**CAC**TATTCCTA	n/a

Table S5. PNA sequences for GFP knockdown experiments. Each PNA sequence was coupled at the N terminus with a cell-penetrating peptide $(KFF)_3K$ and a 2-[2-(2-Aminoethoxy)ethoxy]acetyl linker group. *α-GFP* is designed to knock down GFP in a fluorescent strain of *E. coli* DH5α, while *scr-GFP* and *2MM-GFP* are scrambled and two-mismatch sequences (respectively) to be used as negative controls. Nucleotides in the start codon, as well as PNA bases that complement those nucleotides, are bolded, and mismatched nucleotides are shown in red.

PNA Name	Target Sequence (5' to 3')	PNA Sequence (N to C)
α-GFP	AGGAGAGAAGG**A**	**T**CCTTCTCTCCT
scr-GFP	GAAAAAGGGGGA	TCCCCCTTTTTC
2MM-GFP	AGGA**A**AGA**G**GG**A**	**T**CC**C**TCT**T**TCCT

Table S6. Sequences of ssDNA oligonucleotides designed for the gel shift mobility assay. Oligonucleotides were obtained for each PNA for which antibiotic treatment interaction was observed. Each oligonucleotide is 60 nucleotides long and has a corresponding two-mismatch oligonucleotide, to which the PNA binding is eliminated or drastically reduced. Target sequences are bolded, mismatches in the control oligonucleotides are shown in red.

PNA Name	Binding Oligo	Two-Mismatch Oligo
α-ampC	CAGGCCGTTTTGTATGGAAA**CCAGACCCTATG** TTCAAAATGACGCTCTGCGCCTTATTAA	CAGGCCGTTTTGTATGGAAA**CC<u>C</u>GACC<u>A</u>TATG** TTCAAAATGACGCTCTGCGCCTTATTAA
α-bolA	ACATCTCAGCGTTGTCGGAGGAGATATT**TCAT** **GATGATAC**GTGAGCGGATAGAAGAAAAA	ACATCTCAGCGTTGTCGGAGGAGATATT**TCA<u>G</u>** **GAT<u>T</u>ATAC**GTGAGCGGATAGAAGAAAAA
α-dsrB	AGAAAATCAGCACTCGCGCGCGCCTGGCG**CTG** **CCAGAAAAA**CGAAATTGTTCTACACTGG	AGAAAATCAGCACTCGCGCGCGCCTGGCG**CTG** **<u>A</u>CAG<u>C</u>AAAA**CGAAATTGTTCTACACTGG
α-flhC	AATAAAGTTGGTTATTCTGGG**TGGGAATAATG** **C**ATACCTCCGAGTTGCTGAAACACATTT	AATAAAGTTGGTTATTCTGGG**TGG<u>A</u>AAT<u>G</u>ATG** **C**ATACCTCCGAGTTGCTGAAACACATTT
α-hycA	TGGCATCTCTGTTAAACGGGTAACC**TGACAAT** **GACT**ATTTGGGAAATAAGCGAGAAAGCC	TGGCATCTCTGTTAAACGGGTAACC**TGA<u>G</u>AAT** **<u>C</u>ACT**ATTTGGGAAATAAGCGAGAAAGCC
α-ygaC	GCCCGCGGTTGATAATAACGAGGA**TCAAATAT** **GTAT**TTACGACCAGACGAGGTGGCGCGC	GCCCGCGGTTGATAATAACGAGGA**TCA<u>T</u>ATA<u>A</u>** **GTAT**TTACGACCAGACGAGGTGGCGCGC

SI References

1. T. Wirth, *et al.*, Sex and virulence in Escherichia coli: An evolutionary perspective. *Mol. Microbiol.* **60**, 1136–1151 (2006).
2. M. V. Larsen, *et al.*, Multilocus sequence typing of total-genome-sequenced bacteria. *J. Clin. Microbiol.* **50**, 1355–1361 (2012).
3. F. Jaureguy, *et al.*, Phylogenetic and genomic diversity of human bacteremic Escherichia coli strains. *BMC Genomics* **9**, 560 (2008).
4. G. A. Jacoby, Mechanisms of resistance to quinolones. *Clin. Infect. Dis.* **41**, S120-6 (2005).
5. H. Yoshida, M. Bogaki, M. Nakamura, L. M. Yamanaka, S. Nakamura, Quinolone Resistance-Determining Region in the DNA Gyrase gyrB Gene of Escherichia coli. *Antimicrob. Agents Chemother.* **35**, 1647–1650 (1991).
6. K. L. Hopkins, R. H. Davies, E. J. Threlfall, Mechanisms of quinolone resistance in Escherichia coli and Salmonella: Recent developments. *Int. J. Antimicrob. Agents* **25**, 358–373 (2005).
7. L. Sandegren, A. Lindqvist, G. Kahlmeter, D. I. Andersson, Nitrofurantoin resistance mechanism and fitness cost in Escherichia coli. *J. Antimicrob. Chemother.* **62**, 495–503 (2008).
8. J. Whiteway, *et al.*, Oxygen-insensitive nitroreductases: Analysis of the roles of nfsA and nfsB in development of resistance to 5-nitrofuran derivatives in Escherichia coli. *J. Bacteriol.* **180**, 5529–5539 (1998).
9. D. H. Ezekiel, J. E. Hutchins, Mutations affecting RNA Polymerase associated with Rifampicin Resistance in Escherichia coli. *Nature* **220**, 276–277 (1968).
10. Clinical & Laboratory Standards Institute, “Performance Standards for Antimicrobial Disk Susceptibility Tests; Approved Standard - Twelfth Addition” (2015).